Environmental Monitoring and Assessment (2006) 117: 463–489
DOI: 10.1007/s10661-006-0888-9

URBAN AIR POLLUTION PATTERNS, LAND USE, AND THERMAL LANDSCAPE: AN EXAMINATION OF THE LINKAGE USING GIS

QIHAO WENG[1,*] and SHIHONG YANG[2]
[1]*Associate Professor of Geography, and Director, Center for Urban and Environmental Change, Department of Geography, Geology, and Anthropology, Indiana State University, Terre Haute, IN 47809, USA;* [2]*Department of Geography, South China Normal University, Guangzhou 510630, Guangdong, China*
*(*author for correspondence, e-mail: geweng@isugw.indstate.edu)*

(Received 11 January 2005; accepted 5 July 2005)

Abstract. This article investigates the relationship of local air pollution pattern with urban land use and with urban thermal landscape using a GIS approach. Ambient air quality measurements for sulfur dioxide, nitrogen oxide, carbon monoxide, total suspended particles, and dust level were obtained for Guangzhou City in South China between 1981 and 2000. Landsat TM images and aerial photo derived maps were used to examine city's land use and land cover at different times and changes. Landsat thermal infrared data were employed to compute land surface temperatures and to assess urban thermal patterns. Relationships among the spatial patterns of air pollution, land use, and thermal landscape were sought through GIS and correlation analyses. Results show that the spatial patterns of air pollutants probed were positively correlated with urban built-up density, and with satellite derived land surface temperature values, particularly with measurements taken during the summer. It is suggested that further studies investigate the mechanisms of this linkage, and that remote sensing of air pollution delves into how the energy interacts with the atmosphere and the environment and how sensors see pollutants. Thermal infrared imagery could play a unique role in monitoring and modeling atmospheric pollution.

Keywords: air pollution pattern, Geographic Information System (GIS), Guangzhou, land surface temperature, urban land use

1. Introduction

Urban areas are associated with sources of a variety of air pollutants, and regional pollution problems such as acid rain and photochemical smog. Cities are also major contributors to global air pollution related to ozone depletion and carbon dioxide (CO_2) warming. Within an urban area, the level of pollution varies with the distance to pollution sources, including both stationary and mobile sources (e.g., vehicles). Local pollution patterns in cities are mainly relate to the distribution of different land use and land cover categories, the occurrence of water bodies and parks, building and population densities, the division of functional districts, the layout of transportation network, and air flushing rates. It is well know that pollution levels rise with land use density, which tends to increase towards a city center (Marsh and

Grossa, 2002, p. 224). Therefore, there is generally an urban-rural gradient in the concentrations of air pollutants. For example, the concentrations of particulates, carbon dioxide, and nitrate ion (an oxide, as in acid rain) in the inner city are typically two to three times higher than in the suburban and five times higher than in the rural areas (Marsh and Grossa, 2002, p. 224, Figure 11.12).

Furthermore, urban areas experience another type of pollution – heat pollution. Urban development results in a dramatic alteration of energy balance in the Earth's surface, as natural vegetation is removed and replaced by non-evaporating, non-transpiring surfaces. Under such alteration, the partitioning of incoming solar radiation into fluxes of sensible and latent heat is skewed in favor of increased sensible heat flux as evapotranspirative surfaces are reduced. A higher level of latent heat exchange was found with more vegetated areas, while sensible heat exchange was more favored by sparsely vegetated such as urban impervious areas (Oke, 1982). Therefore, urban areas generally have higher solar radiation absorption and a greater thermal capacity and conductivity. This thermal difference, in conjunction with waste heat released from urban houses, transportation, and industry, contribute to the development of an urban heat island (UHI). Because of construction of tall and closely spaced buildings, the flushing capability of the air at the ground level is largely reduced.

Thermal variations within an urban area mainly relate to different land use and land cover classes, surface materials, and air flushing rates (Marsh and Grossa, 2002, p. 227). Each component surface in urban landscapes (e.g., lawn, parking lot, road, building, cemetery, and garden) exhibits a unique radiative, thermal, moisture, and aerodynamic properties, and relates to their surrounding site environment (Oke, 1982). Because of its significance, recent literature has witnessed a growing interest in the relationship between land use/cover (vegetation) and land surface temperature (LST) (e.g., Carson *et al.*, 1994; Gallo and Owen, 1998; Gillies and Carlson, 1995; Gillies *et al.*, 1997; Goward *et al.*, 2002; Weng, 2001, 2003). Remote sensing data have been employed to measure LST and study urban thermal variations, including NOAA AVHRR data (Kidder and Wu, 1987; Balling and Brazell, 1988; Roth *et al.*, 1989; Gallo *et al.*, 1993; Streutker, 2002, 2003), Landsat TM and ETM+ (Carnahan and Larson, 1990; Kim, 1992; Nichol, 1994, 1996; Weng, 2001, 2003; Weng *et al.*, 2004), and ATLAS data (Quattrochi and Ridd, 1994; Quattrochi and Luvall, 1999). Studies using satellite-derived radiant temperature have been termed as the surface temperature heat islands (Streutker, 2002). LST is believed to correspond more closely with the urban canopy layer heat islands, although a precise transfer function between LST and the near ground air temperature is not yet available (Nichol, 1994). Byrne (1979) has observed a difference as much as 20 °C between the air temperature and the warmer surface temperature of dry ground.

The relationship between air pollution and urban heat (and thus UHIs) is not clearly understood, although both relate to the pattern of urban land use and land cover. UHIs favor the development of air pollution problem, but are not an

indicator of air pollution (Ward and Baleynaud, 1999). It is known that higher urban temperatures generally result in higher ozone levels due to an increased ground-level ozone production (DeWitt and Brennan, 2001). Moreover, higher urban temperatures mean increased energy use, mostly due to a greater demand for air conditioning. As power plants burn more fossil fuels, pollution level is driven up. A few studies have so far examined the correlation between LST and air pollution measurements. Poli *et al.* (1994) investigated the relationship between satellite derived apparent temperatures and daily sums of total suspended particulates (TSP) and sulphur dioxide (SO_2) in the winter season in five locations of Rome, Italy. It is found that apparent temperatures had a strong negative correlation with TSP, but a weak correlation with SO_2. Brivio *et al.* (1995) used three AVHRR images of Milan, Italy, acquired on February 12–14, 1993, to study the correlation of apparent temperatures with air quality parameters including TPS and SO_2. A weak correlation was discovered with both TPS and SO_2, which could be explained by the large pixel size of the image. Ward and Baleynaud (1999) explored the correlation between Landsat TM band 6 digital counts and the concentrations of pollutants, including black particulates (BP), SO_2, nitrogen dioxide (NO_2), nitrogen monoxide (NO), strong acidity (AF) in Nates, France, based on the measurements of daily sums, individual measurements of every 15 minutes, and daily mean values taken on May 22, 1992. It is found that apparent temperatures were highly positively correlated with BP, moderately correlated with SO_2 and daily means of NO_2, NO, and AF, but weakly correlated with instantaneous measurements of NO_2 and NO. These studies contribute to the current literature by adding more evidence on the correlation between air pollution and urban thermal patterns. However, none of these studies have fully utilized the state-of-the-art technologies of satellite remote sensing and GIS, which have been proved to be most appropriate and effective for handling spatial data such as urban air pollution, urban heat, and land use/cover patterns. Current remote sensing technology allows for obtaining a reasonably high quality of LST estimates through various stages of correction process (Voogt and Oke, 2003). GIS technology provides a flexible environment for entering digital data from various sources, and is a powerful tool in analyzing numerical relationships within and among map layers. It is advantageous that an integrated approach of remote sensing and GIS can be developed and applied when examining the relationships among spatial variables such as urban land use, pollution, and thermal variation within an urban context.

The objective of this study is to investigate local air pollution patterns in Guangzhou in the period of 1980 to 2000, and to examine the relationship of the air pollution patterns with land use and land cover changes, and urban thermal landscapes. This coastal city in South China has undergone a fundamental change in land use and land cover due to accelerated economic development under the reform policies since 1978. Because of less attention paid onto urban air quality, and the lack of appropriate land use planning and the measures for sustainable development, economic development and rampant urban growth has created severe

negative environmental consequences. Specific questions will be addressed in this paper include: (1) how has local air pollution pattern changed over the past two decades?; (2) how has urban growth altered the air pollution pattern and promoted the UHI effect as indicated by satellite derived LST measurements?; and (3) how did the pollution patterns relate to urban land uses and to urban thermal patterns? Detailed information on the relationships among these three spatial variables in an urban area would be valuable to urban and environmental planners. Knowledge on their relationships can be used by planners to evaluate the need for new or revised urban design and landscaping policies for mitigating the adverse environmental effects of building mass, transportation networks, and poor landscape layouts.

2. Study Area: Guangzhou, China

Guangzhou (also known as Canton) is located at latitude 23°08′ N and longitude 113°17′ E and lies at the confluence of two navigable rivers of the Zhujiang

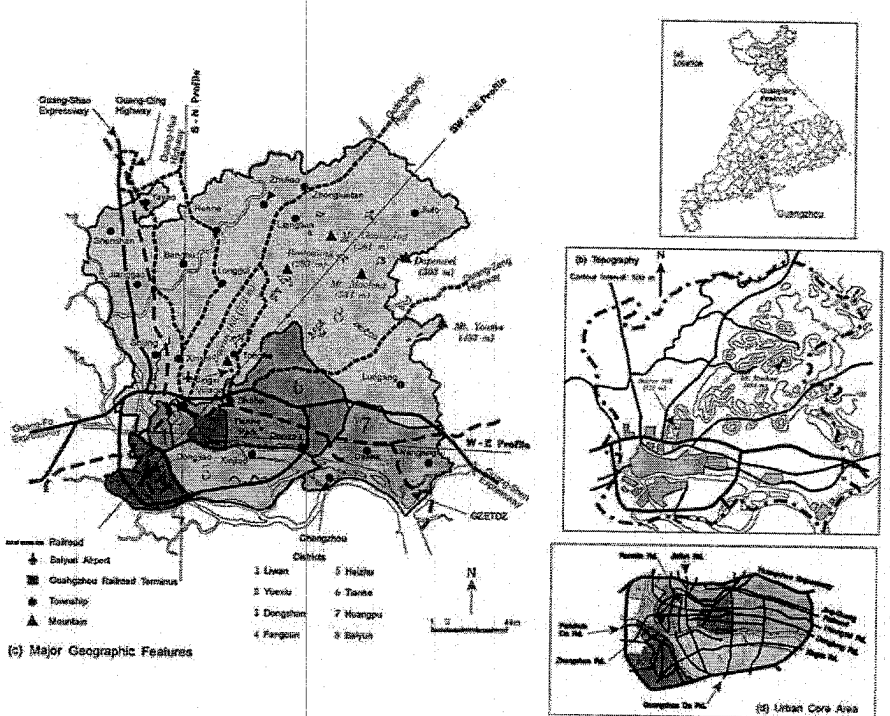

Figure 1. Study area map showing major geographic features and the eight districts, with inset maps of location and the urban core area.

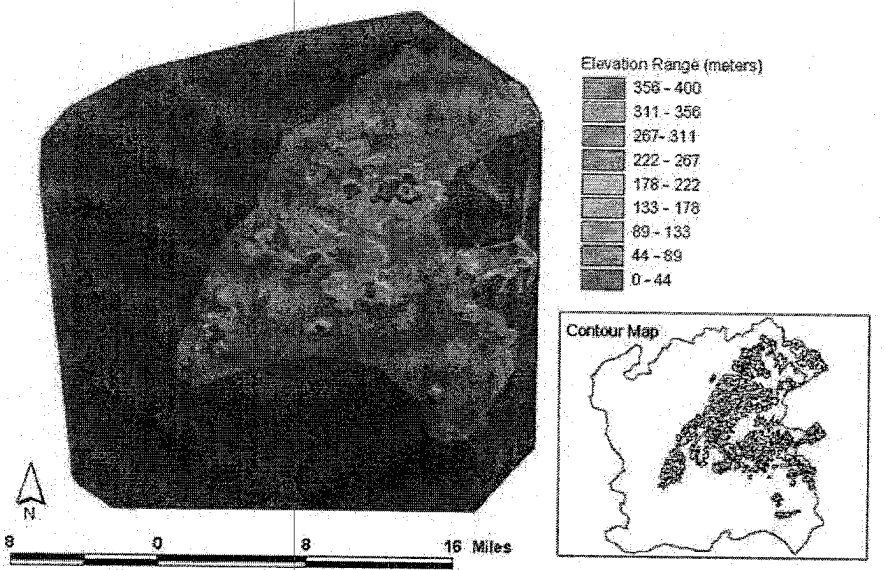

Figure 2. Digital elevation model of Guangzhou (inset: contour map of Guangzhou).

River (literally the "Pearl River") system (Figure 1). With a population of 3.99 million and total area of 1,444 square kilometers (Guangdong Statistical Bureau, 1999), it is the sixth most populous city in the nation. It has been the most important political, economic, and cultural center in South China. The Guangzhou municipality comprises eight administrative districts in the city proper (Figure 1), and four rural counties. This study focuses on the city proper. It has a subtropical climate with an average annual temperature of 22 °C, with the lowest temperature in January (averaging 18.3 °C) and the highest temperature in July (averaging 32.6 °C) (computed based on averages of the daily mean temperatures). The annual average precipitation ranges from 1600 to 2600 mm. Because of the impact of the East Asian and Indian monsoonal circulation, about 80% of the rainfall comes in the period of April to September with highest concentration in spring. The humidity is high in all seasons, and the average relative humidity is 80 percent. This stems principally from the wetland environment and the basin-like terrain of the city (Figure 2). Guangzhou has a history of urban development spanning across 2,000 years (Xu, 1990). The urban development has progressed at an unprecedented pace, especially after the implementation of economic reforms in 1978, with dominant expansions toward the east and the north. The total area of finished housing covered only 12.3 square kilometers in 1949 when the People's Republic of China was founded, but increased to 127.9 square kilometers in 1999.

3. Data Acquisition and Analysis

3.1. AMBIENT AIR QUALITY

In Guangzhou, ambient air quality was monitored through six municipal monitoring stations (the number of monitoring stations was increased to nine after 1996). The concentrations of pollutants, sulfur dioxide (SO_2), nitrogen oxides (NO_x, consisting of NO and NO_2), carbon monoxide (CO), total suspended particles (TSP), as well as dust level, are routinely measured in the stations. These measurements are analyzed with the standard methods stipulated by the State Environmental Protection Administration (SEPA) of China. Concentrations of SO_2 were collected by using the designated impinger (GS-3) that was calibrated for each measurement with bubble flow meters, and were analyzed by the method of pulse fluorescence. Concentrations of NO_X were measured by using the NO_X impinger, and then analyzed by the method of chemical fluorescence. TSP concentrations were sampled using the KB-120E samplers that were calibrated quarterly with orifice plate meters, and were determined by the method of filter lightening. Concentrations of CO were measured by the method of infrared absorption. The six monitoring stations are nationally regulated ones, locating in various functional districts of land use: industrial, commercial, mixed urban uses, dense transportation, residential, and sanitary suburban areas. Data for the monitoring stations were strictly restricted to internal uses, but this research was able to collect the city's mean measurements of the pollutants since the 1980s through compiling a time series of environmental quality reports in an attempt to analyze the temporal change of air quality. Table I shows annual means of concentrations of the above pollutants every five years and the national air quality standards for these pollutants. Moreover, geographic distribution maps of SO_2, NO_x, TSP, and dust level included in *Guangzhou Natural Resources Atlas* (Guangzhou Municipality Planning Committee, 1997) were manually digitized and converted into GIS data layers, so that the spatial patterns of air pollution can also be examined. The maps were produced by the city's environmental monitoring

TABLE I
Annual means of concentrations of the air pollutants observed in major years

Pollutants	1980	1985	1990	1995	2000	NAQS for residential areas
SO_2 (mg/m^3)	0.09	0.089	0.097	0.057	0.045	0.06
NO_x (mg/m^3)	0.04	0.073	0.137	0.123	0.061	0.10
TSP (mg/m^3)	0.24	0.226	0.22	0.31	0.157	0.20
Dust (ton/km^2. month)	15.94	12.7	9.56	9.16	7.34	6-8
CO (mg/m^3)	No data	2.8	3.16	2.91	No data	4.00

Note: NAQS – national air quality standard.

authority based on data collected in the fixed monitoring stations between 1983 and 1992 in conjunction with the results of several mobile studies. The placements of contours in these maps have a fairly high accuracy, and are thus appropriate for this type of analysis.

3.2. Land use and land cover

The source data for mapping urban and built-up areas include a topographic map, a land use and land cover map, and satellite imagery. The topographic map was produced by the Chinese government in 1960, based on 1:25,000 aerial photographs taken in 1958. The land use and land cover map was prepared by the Department of Geography, Zhongshan University, based on aerial photographs taken in 1984. The two maps have the same scale of 1: 50,000. Urban and built-up areas were delineated from the two maps, and manually digitized into computer with ArcInfo computer program.

The satellite images are two Landsat Thematic Mapper (TM) images, dated on December 13, 1989, and August 29, 1997 respectively. Each Landsat image was rectified to a common UTM coordinate system based on 1:50,000 scale topographic maps. These images were resampled using the nearest neighbor algorithm, with a pixel size of 30 m for all bands. The resultant root mean squared error was found to be 0.77 pixel (or 23.1 m on the ground) for the 1989 image, 0.58 pixel (or 17.4 m on the ground) for the 1997 image.

Land use and land cover patterns for 1989 and 1997 were mapped using Landsat TM data. A modified version of the Anderson scheme of land use/cover classification was adopted (Anderson *et al.*, 1976). The categories include: (1) urban or built-up land, (2) barren land, (3) cropland (rice), (4) horticulture farms (primarily fruit trees), (5) dike-pond land, (6) forest, and (7) water. A supervised signature extraction with the maximum likelihood algorithm was employed to classify the Landsat images. Both statistical and graphical analyses of feature selection were conducted, and bands 2, 3, and 5 were found to be most effective in discriminating each class and therefore were used for classification. The accuracy of the classified maps was checked with a stratified random sampling method, by which 50 samples were selected for each land use and land cover category. The reference data was collected from field survey or from existing land use and cover maps that have been field-checked. Large-scale aerial photographs were also employed as reference data in accuracy assessment when necessary. The overall accuracy of classification was determined to be 90.57 percent, and 85.43 percent respectively. The KAPPA index was 0.8905 for the 1989 map and 0.8317 for the 1997 map. A detailed accuracy assessment result, including the error matrices and the user's and producer's accuracy of the land use and land cover maps, can be found in Weng (2001). The urban and built-up areas were extracted from each land use and land cover map to create the urban maps.

3.3. LAND SURFACE TEMPERATURES

LSTs were derived from geometrically corrected Landsat TM thermal infrared bands dated on December 13, 1989 and August 29, 1997. The TM thermal band has a spatial resolution of 120 meters and a noise level equivalent to a temperature difference of 0.5 °C (Gibbons and Wukelic, 1989). The local time of satellite overpass was in the morning (approximately 10:00 A.M.), so that the chance for detecting a weaken UHI is maximized. Since both images were acquired at approximately the same time, a comparative study is feasible. A quadratic model was used to convert the digital number (DN) into radiant temperatures ($T_{(k)} = 209.831 + 0.834DN - 0.00133DN^2$) (Malaret *et al.*, 1985). Temperature values obtained were then corrected with emissivity (ε) according to the nature of land cover. Vegetated areas were assigned a value of 0.95 and non-vegetated areas 0.92 (Nichol, 1994). The differentiation between vegetated and non-vegetated areas was made according to the normalized difference vegetation index (NDVI) values, which were computed from visible (0.63–0.69 μm) and near-infrared (0.76–0.90 μm) data of TM images. The emissivity corrected LSTs were computed using the equation developed by Artis and Carnhan (1982):

$$\mathrm{LST} = \frac{T_{(k)}}{1 + \left(\lambda * T_{(k)}/\rho\right) \ln \varepsilon} \tag{1}$$

where: λ = wavelength of emitted radiance (for which the peak response and the average of the limiting wavelengths ($\lambda = 11.5$ μm) (Markham and Barker, 1985) will be used), $\rho = h * c/\sigma (1.438 * 10^{-2}$ mK), σ = Boltzmann's constant ($1.38 * 10^{-23}$ J/K), h = Planck's constant ($6.626 * 10^{-34}$ J sec), and c = velocity of light ($2.998 * 10^8$ m/sec).

4. Air Pollution Patterns

4.1. SO_2

Guangzhou's air quality was getting worse after the 1970s, and became a major concern after the 1980s with an accelerated urbanization and industrialization. Figure 3(a–e) shows inter- year variations in annual mean concentrations of SO_2, NO_x, TSP, dust level, and CO from 1981 to 2000. The concentration of SO_2 continued to go up after 1981, peaked at 1989, and then gradually declined. The year of 1992 witnessed a long-awaited victory, when the Chinese national air quality standard (NAQS) for SO_2 for residential areas, 0.06 mg/m^3, was not exceeded for the first time since 1972 (GZCLCCC, 1995, pp. 612–613). Figure 3a indicates that there was an elevated peak of SO_2 concentration between 1996 and 1998, however. The three years had all exceeded the NAQS, but marginally in 1996

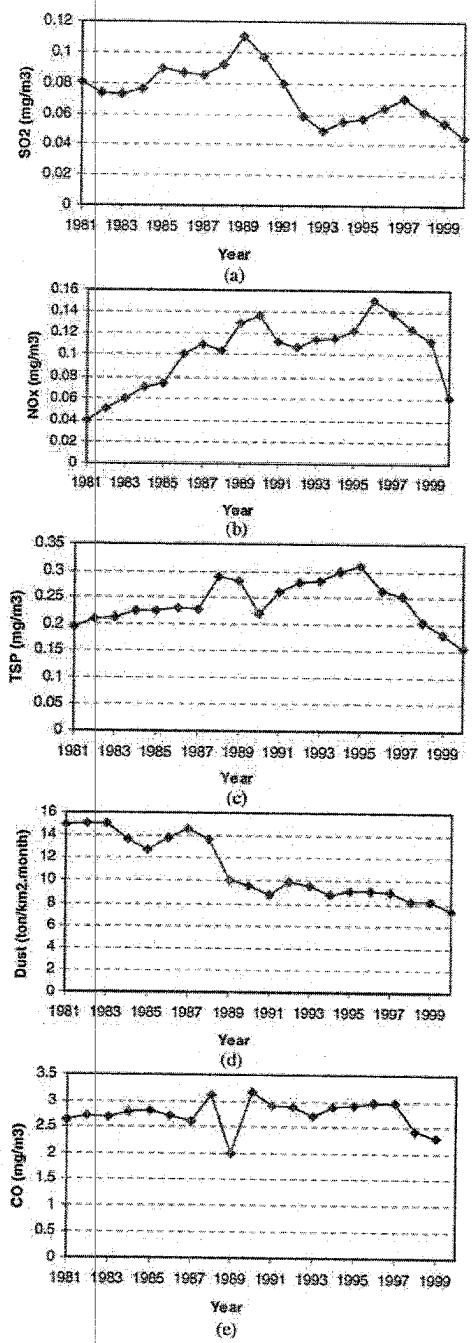

Figure 3. Yearly variations of annual mean concentrations of SO_2, NO_x, TSP, dust level, and CO, 1981-2000.

(0.064 mg/m^3) and 1998 (0.061 mg/m^3) while remarkably in 1997 (0.07 mg/m^3). The intra-year variation was characterized a higher level of concentration in the winter months and a lower level in the summer months (Xie and Chen, 2001). This seasonal pattern was not evident owing to slight seasonal variations of the temperatures.

The level of SO_2 concentration was largely related to the industrial use of coal as a major energy source, and the use of coal combustion for cooking and heating in catering industry and households. As a result, areas with industrial plants, high population density, and clustering of catering industry tended to have a high concentration of SO_2. Figure 4a shows two focal points of contamination, one locating in Liwan District, and the other around Yuanchun township of Tianhe District. Liwan was home to the city's electricity generation plant, and the abnormally high SO_2 concentrations can also be attributed to the biggest concentration of catering enterprises in the city, and extremely high building and population densities. In contrast, Tianhe District did not have a high population density neither a clustering of catering enterprises. However, it possessed sparsely distributed but highly polluted industries, especially chemical plants. Away from these "pollution hubs", SO_2 concentration gradually decreased. An intra-city gradient was apparently detected, if we look beyond the old city core (i.e., Yuexiu, Dongshan, and Liwan Districts) and Tianhe towards the northern part of the city. The majority of Baiyun District had kept relatively clean, with a concentration level below 0.02 mg/m^3. Research conducted by Xie and Chen (2001) of Guangzhou Environmental Monitoring Station suggests that SO_2 measurements in the sanitary suburban station, which is located at the southern slope of Baiyun Hill, showed a highly similar temporal variation pattern as those in other functional districts. The urban-rural disparity was narrowed down during the period of 1985 to 1997, from 0.09 mg/m^3 in 1985 to 0.067 mg/m^3 in 1989, with a sharp decrease in 1993 to 0.026 mg/m^3, leveling down in 1997 to 0.018 mg/m^3.

Since 1990, the urban Guangzhou had been able to gradually lower the overall level of SO_2 contamination due to the following three reasons. First, a substantial number of high polluting enterprises were forced to close down or relocated away from the urban core area. Second, new technologies were applied to reduce the amount of SO_2 emission. Finally, use of liquefied petroleum gas increased rapidly (Figure 5), replacing coal to become the nearly sole source of energy in catering and home uses. These improvements, however, were somewhat counterbalanced by a sizeable increase of industrial use of coal (Figure 5), resulted from an accelerated industrial development in the 1990s. Furthermore, many lately built electricity generation plants in the Zhujiang Delta, where Guangzhou is located, became new sources of air pollution through dominant southeasterlies in the summer. As a result, although the overall concentration level had dropped, the impacted area of SO_2 pollution showed an increasing tendency of dispersal (Xie and Chen, 2001).

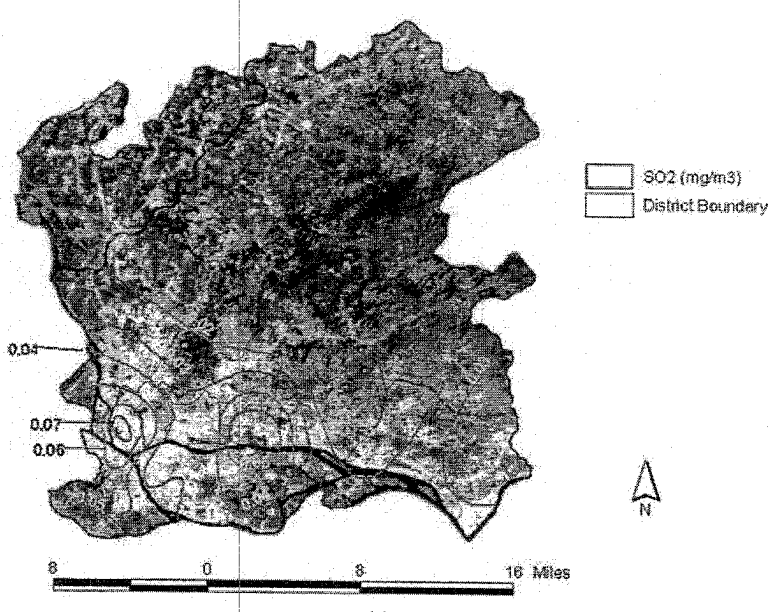

(a)

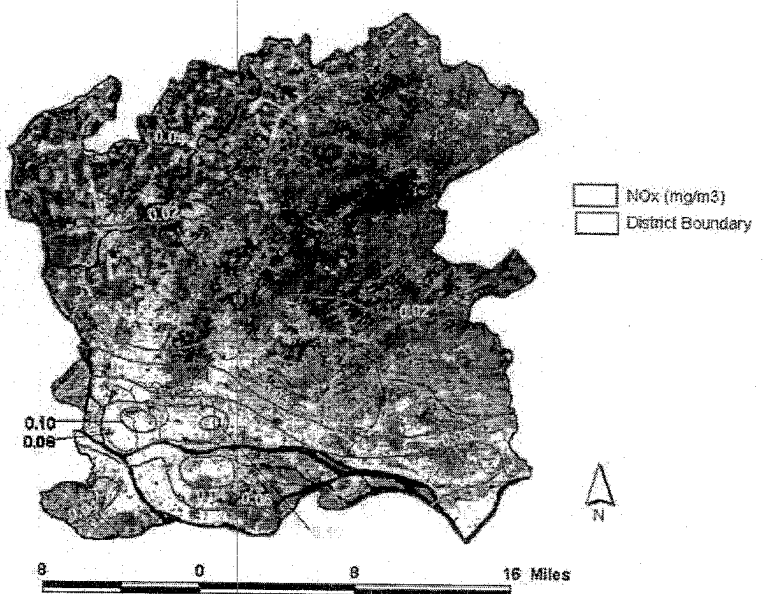

(b)

Figure 4. Geographical distribution of the concentrations of major air pollutants in Guangzhou. Contours are interpolated from point data observed in the monitoring stations. Data represent annual averages of pollutant measurements. The base map is land surface temperature map of August 29, 1997 derived from Landsat TM thermal infrared data. (*Continued on next page*)

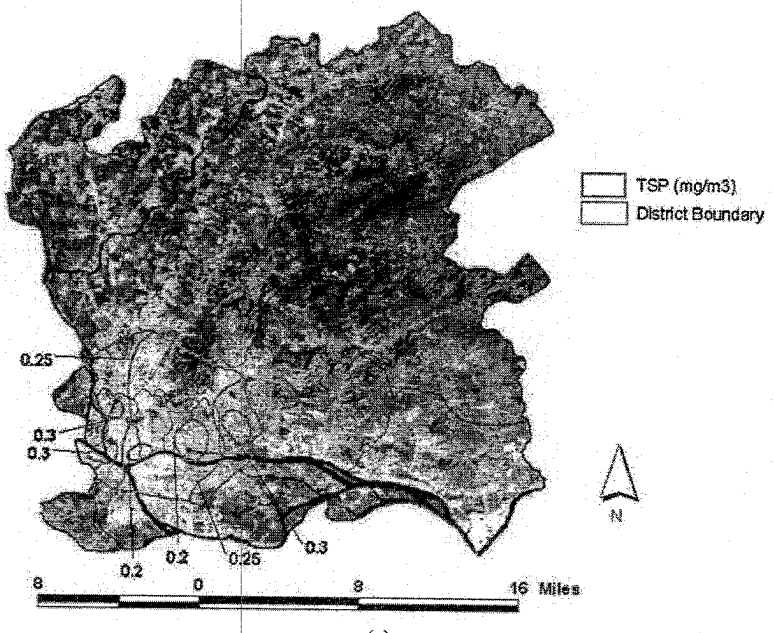

(c)

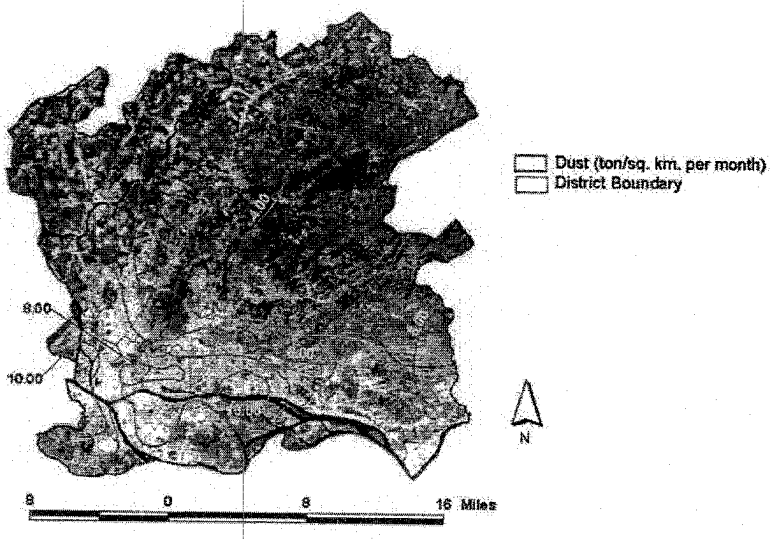

(d)

Figure 4. (*Continued*)

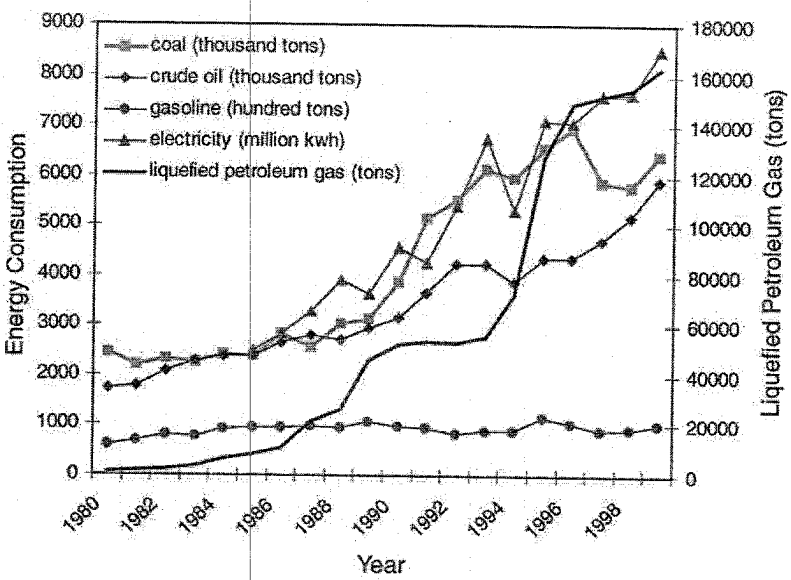

Figure 5. Structural changes in energy consumption in Guangzhou, 1980–1999 (Source: Guangzhou Statistical Bureau, 1999).

4.2. NO_x

Ambient NO_x concentrations showed a trend of wavily increase to the peak in 1996, and then gradually decreased (Figure 3b). According to Chinese NAQS for NO_x, i.e., 0.1mg/m^3 for residential areas, the city as a whole had exceeded the standard for all the years from 1986 to 1999. In many of the years observed, the city possessed the highest concentration level among all Chinese cities (Zhang *et al.*, 1999; Wang *et al.*, 2001). The intra-year variation was not as large as that of SO_2, although a slightly higher level of concentration in the winter months were observable (Xie and Chen, 2001). Researches reveal that this pollution problem was strongly related to the rapid growth of vehicular exhaust emission (Zhang *et al.*, 1999; Wang *et al.*, 2001; Qian *et al.*, 2001). Between 1981 and 1999, the number of cars in the city increased from 26,153 to 273,036, yielding an annual increase rate of 13.92 percent (Figure 6). The number of motorcycles exhibited a similar rate of increment. The city possessed 157,677 motorcycles in 1990, but elevated to 385,508 in 1999, yielding an annual rate of 10.44 percent (Figure 6). Traditional dependency of civil transportation on bicycles had been impaired, as household possession of motorcycles increased drastically (from 4 per hundred households in 1990 to 23.2 in 1999), while the number of bicycles per hundred households decreased from 191.7 to 160.6 during the same period of time (Figure 6). The massive volumes of vehicles, in conjunction with poor vehicle and fuel quality

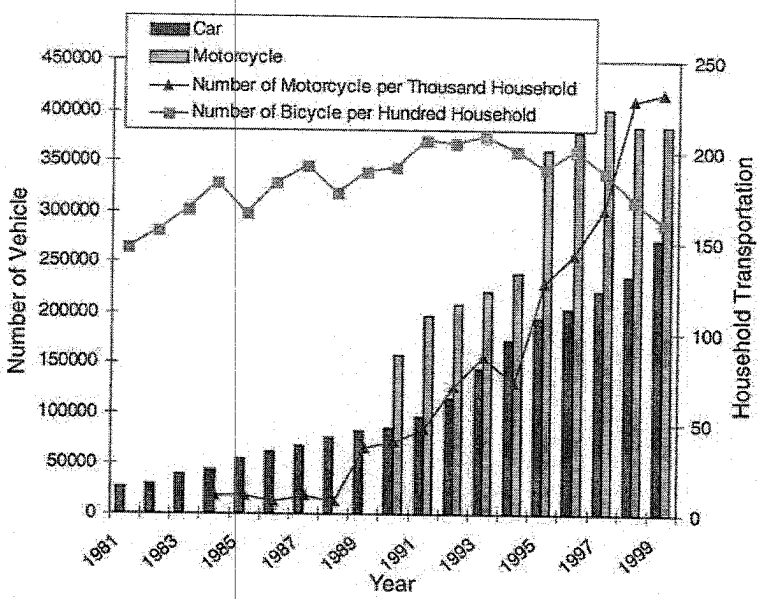

Figure 6. Changes in public transportation (cars, motorcycles, and bicycles), 1980–1999 (Source: Guangzhou Statistical Bureau, 1999).

with no catalytic converters, produced a high volume of pollutants including NO_x and CO. Moreover, the city's road construction and pavement management did not keep up with the speedy growth of vehicle population. The total area of paved roads was 3.6 sq. km. in 1981, and rose to 25.56 sq. km. in 1999 (Guangzhou Statistical Bureau, 1999), with an annual rate of 11.5 percent. This increment rate, however, was clearly lower than the rate of vehicle increase, which contributed to heavy traffic congestion in most of the time. Low driving speed, high idle, and frequent acceleration caused automobile engines to be less efficient combustors, and to become a main source of air pollution. Consequently, NO_x concentrations were much higher in dense traffic areas. Highway corridors and urban street canyons were notorious for severe levels of NO_x pollution, such as Dongfeng Road, Jiefang Road, and Huangshi Road (Figure 1d) (Zhang *et al.*, 1999; Xie and Chen, 2001).

Figure 4b shows that two areas exhibited the highest level of NO_x concentration (≥ 1.0 mg/m^3), one in Yuexiu District and the other smaller one in the eastern part of Dongshan District. Both were directly related to extremely heavy traffic and impaired air circulation. As distance increased from the pollution hubs, the level of NO_x concentration went down gradually. A comparison of Figure 4b with Figure 1c reveals that the spatial pattern of NO_x concentration was highly correlated with the pattern of the city's transportation network. This is particularly true when both patterns were viewed and referenced to the eastward expansion of urban

development. The south–north intra-city gradient was apparently observed, which reflected changes in the density of transportation network and building density. The old city core (Liwan, Yuexie and Dongshan Districts) in the south discovered the highest NO_x concentration, leveling down to Tianhe District and reaching the lowest concentration in the District of Baiyun in the north. The old city core not only held an extremely high density of transportation network, but also the highest building density. High and closed-spaced buildings in these districts had caused flushing of polluted surface air to be slow and incomplete. Haizhu and Huangpu Districts found an intermediate level of NO_x concentration due to high building density and moderate traffic. Similar to ambient SO_2 concentrations, NO_x concentrations in the sanitary rural areas rose quicker than those in the urban areas, leading to a smaller urban-rural gradient (Xie and Chen, 2001).

There was a general decline trend in the NO_x concentration since 1996 (Figure 3b). Numerous laws and regulations were implemented to tighten up vehicular emission control, and to mandate road checks and installation of purification equipment. A series of emission reduction products were introduced, as well as mandatory use of unlead gasoline after July 2000. Motorcycles and smoky cars were regarded to be especially problematic; hence, the city government stepped up to set up a series of regulations for emission control. Finally, the city government had advocated the adoption of environmentally conservative vehicles, which used liquefied petroleum gas, electricity, or other sources of "clean" energy. The data we collected for this study indicate the above measures had been effective.

4.3. TSP

Aside from the two major pollutants (SO_2 and NO_x), TSP is another regulated pollutant measured in the monitoring stations. Figure 3c illustrates the temporal changes in the concentration of TSP between 1981 and 2000. It is clear that TSP concentration kept a trend of increase until reached the peak in 1995, and then declined. According to Chinese annual mean standard for residential areas of 0.2 mg/m^3, Guangzhou had seventeen years (from 1982 to 1998) out of the twenty observed exceeding the standard. Only years 1981, 1999, and 2000 were below the NAQS. Seasonal variations in TSP were stronger than those in SO_2 and NO_x. TSP levels, as indicated by monthly arithmetic means, were higher in the wintertime (November through March), which may be attributed to a slightly increase of domestic fuel combustion (Qian *et al.*, 2001).

Spatially, TSP concentrations were remarkably uneven, showing a great urban-rural gradient. Figure 4c shows that two north-south corridors of high concentration can be observed. The western corridor extended from Xinshi Township of Baiyun District, crossed the Pearl River, and to near Dongdun Township of Fangchun District. The eastern corridor set out from Guangzhou East Railroad Station, passed the Pearl River, and arrived at Xinjiao Township of Haizhu District. Within these two corridors, TSP concentration was always higher than 0.25 mg/m^3, with some

"spots" bearing even higher levels of concentrations. In between the corridors, TSP concentration ranged from 0.15 to 0.25 mg/m^3, but some areas may be cleaner than others. Because no measurements were available to map TSP distribution for the whole city, Huangpu District and most areas in Baiyun, Tianhe, Haizhu, and Fangcun Districts were left out. Presumably, TSP concentrations in these areas were lower than the areas mapped, since there were a higher density of transportation network and population, and several highly polluted plants in the urban core area.

4.4. Dust

The dust level appeared to climb up continually in the 1970s. In 1971, the city's average dust level was 16.3 ton per square kilometer per month (GZCLCCC, 1995, p. 612). The level was escalated to 20.4 ton during the period between 1972 and 1978. Large spatial disparity existed among different functional districts of industrial, commercial, residential, and sanitary rural areas, with an average dust level of 33.4, 20.2, 20.4, and 7 ton respectively (GZCLCCC, 1995, p. 612). In 1979, monthly dust level decreased to 19 ton per square kilometer (GZCLCCC, 1995, p. 613). Figure 3d reveals that this declining trend persisted throughout the study period from 1981 to 2000, in spite of some "ups and downs" in the plot. This general trend of decline did not mean that Guangzhou had become a "clean" city. Instead, all of the years observed, except for 2000, exceeded the Chinese NAQS for dust level, which is 6.0–8.0 ton for residential areas. The main sources of dust were plants and thousands of construction sites (over 3000 in the early 1990s) in the city (Guangzhou Bureau of City Planning, 1996).

Figure 4d shows the spatial distribution of dust concentration in 1992. There were two dust pollution centers (both exceeded 10 ton/sq. km per month), with one located in Liwan District, and the other located in Yuanchun industrial township of Tianhe District. Both Guangzhou Concrete Plant and Xichun Electricity Power Plant had had a great impact on the high dust level in Liwan District. Yuexiu, Dongshan, Haizhu, and Tianhe Districts were next to Liwan in terms of the concentration level. Baiyun District detected the lowest dust level. Contour lines of Figure 4d illustrate an overall spatial pattern, i.e., the dust level decreased from the southwestern to the northeastern part of the city.

4.5. CO

Figure 3e shows that CO concentration kept relatively stable during the observed years, ranging from 2.0 to 3.16 mg/m^3. The CO concentration measurements had not exceeded the Chinese NAQS for residential areas, which is 4.0 mg/m^3. The levels of CO concentrations were mainly related to vehicular emission. Research indicates that 84.8% of the total CO in the atmosphere was resulted from the emission of vehicles in 1994 (Zhang *et al.*, 1999). Accordingly, the geographic distribution of CO

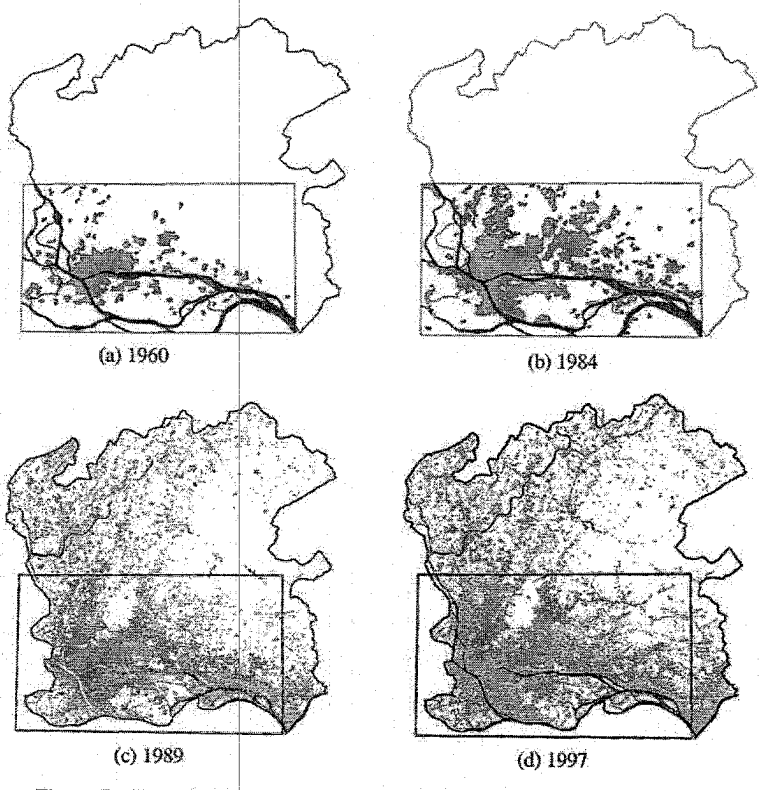

Figure 7. Changes in urban and built-up land use in Guangzhou, 1960–1997.

concentration was traffic related. The concentrations were extremely high in dense traffic areas such as urban street canyons and highway corridors. A diffusion experiment conducted by Zhang *et al.*, during July 14 and August 10, 1998, suggested that CO concentration in Dongfeng Street reached as high as 72.1 mg/m^3, with an average of 9.0 mg/m^3. The level of concentration fluctuated with traffic flow, and was higher between 7:00 A.M. and 9:00 P.M. (Zhang *et al.*, 1999). The leeward side of a street usually had CO concentrations about twice higher than those observed at the windward side, due to wind vortices that carried the pollutant to the leeward side and ascended to the leeward roof edge (Xie *et al.*, 2003). Like NO_x, the old city core (Liwan, Yuexie and Dongshan Districts) displayed a higher CO concentration because of dense transportation networks and closely space buildings.

5. Urban Land Use and Air Pollution Patterns

Guangzhou city proper has experienced a series of drastic changes in the administrative boundaries. These changes affect the computation of urban and built-up areas in different periods of time. The current city jurisdiction came into effect

in 1988, governing eight urban districts and four adjacent counties. The 1960 and 1984 urban maps cover the urban core area only. The remote sensing-GIS analysis indicates that the urban and built-up land had expanded by more than six times from 1960 to1997. In 1960, the urban and built-up area was 64.2 sq. km (Figure 7a) and 159.6 sq. km in 1984 (Figure 7b). During this 24-year period, urban land use (in the rectangular box) increased by 95.4 sq. km, or by 149 percent. The rectangular box defines the limit of the 1984 aerial photograph survey, which lies between 23°2′30″ and 23°13′40″ N in latitude and 113°10′00″ and 113°34′00″ E in longitude, covering the then urban area. Moreover, the land use and land cover maps derived from the Landsat TM images show that the urban and built-up area was 194.8 sq. km in 1989 (Figure 7c) and 295.2 sq. km in 1997 (Figure 7d). Urban land use increased by 100.4 sq. km, or by 51.5 percents in the eight-year period. Overlaying the urban land use maps with a city district boundary and major roads reveals the areal extent and spatial occurrence of urban and built-up areas and the expansion trend.

Before the communist took over in 1949, there was an old city core area (the biggest polygon in Figure 7a) extending from the Haizhu Bridge to some narrow and crowed streets in the Yuexiu and Dongshan Districts. Most of the new developments took place in the suburbs as organized clusters for accommodating industries, warehouses, or external transportation facilities, aside from a few developments on the outskirts of the old city core (Xu, 1985). Huangpu was designated as the out port of the city. New developments were directed to the suburbs in order to contain the growth of the inner city. When a project required a large piece of land, city planners would intentionally locate it in a remote area that had sufficient, less productive land, especially in the eastern and southern suburbs. The built-up area increased from 36 sq. km in 1949 to 56.2 sq. km in 1954 (Guo, 2001). In the late 1950s, there was a significant increment in industrial and residential land uses. Factories were built in selected areas of Haizhu, Fangcun, and Huangpu Districts, while residential developments spread out in the Tianhe District to house higher education, research, and medical units.

During the 1960s and 1970s, urban development was sluggish due to continuous political movements. New factories were built in the Haizhu District, and production and port facilities were expanded to the northeast riverbank of Fungcun District. The city's port function started to shift largely to Huangpu District, where heavy chemical and power industries had been initiated. The stature that Guangzhou was sanctioned as the only foreign trade center in the pre-reform China warranted new housing developments on the northern fringe of Yuexiu District. In addition, a major railway terminus was developed immediately north to the old city core. These developments promoted the city's northern and northwestern expansion. By 1978, the total built- up area reached 89 sq. km.

The 1980s witnessed a dramatic urban development. A triangular Economic and Technological Development Zone (9.6 sq. km) was established in Huangpu District to attract foreign investment in industries. The Huangpu New Port finished

building up eight 20,000 tonnage deepwater berths for ships. These constructions, in conjunction with other port facilities, residential and office buildings, hotels, schools, recreational facilities, shaped a modern Huangpu District. Furthermore, the Baiyun International Airport was reconstructed and expanded. New bridges were constructed to link with the island of Ho Nam (*Henan*), laying the foundation for future southern expansion. Figure 7c shows that two urban development corridors were becoming visible in 1989, one expanding eastward to Huangpu, and the other expanding northward along the expressways.

The urban and built-up areas grew even faster in the 1990s, primarily owning to the development of commercial housing. Commercial housing was initially scattered out in Tianhe District. However, recent development shifted to the northern and southern banks of the Zhujiang. A modern business and residential zone of 6.6 sq. km, i.e., Zhujiang New Town (*Zhujiang Xin Cheng*), was developed along the northern waterfronts of the Zhujiang immediately east to the old city core. In terms of industrial land use, there had been substantial developments in Tianhe High-Tech Industrial Park, while heavy industries continued to build up in Huangpu District. By 1997, the urban and built-up area reached 295.2 sq. km. Figure 7d shows that a west–east-running urban corridor following the northern shore of the waterway has taken shape. In addition, northward urban sprawl along both sides of Baiyun Hill is now conspicuous feature in the city's land use.

How has the urban growth and associated land use/cover changes altered the local air pollution pattern in Guangzhou? To answer this question, several GIS analyses were implemented using the following procedures. First, using the buffer function in GIS, three GIS data layers were constructed. The first buffer shows ten buffer zones around the major roads in the city (the road buffer, hereafter), each with a width of 1000 meters. The second and third buffer layers were created to delineate ten buffer zones around the geometric center of Liwan District (the Liwan buffer, hereafter) and Yuanchun Township of Tianhe District (the Yuanchun buffer, hereafter), each having a width of 1000 meters (Figure 8). As has been discussed in Section 4, the proximity to the major roads or the pollution centers has been determined to have an important implication in local air pollution patterns. Second, the urban map of 1989 (Figure 7c) was overlaid with each buffer layer one-by-one to calculate the amount of urban/built-up land in each buffer zone. The density of urban/built-up was then calculated by dividing the amount of urban/built-up land by the total land area in each zone. The 1989 urban map was used because it matched best the year (1992) when data were collected to create the pollution maps. Finally, each of the concentration maps (SO_2, NO_x, and Dust) (Figures 4a, b, c) were overlaid with each of the buffer maps, so that the value of concentration in each buffer zone can be calculated. The concentration map of TSP (Figure 4c) was excluded in these GIS analyses, since no sufficient data was obtained to cover the whole city proper.

For each pollutant, three correlation analyses were conducted between the densities of urban/built-up land in each buffer zone and the mean values of concentration.

TABLE II

Correlation coefficients between pollutant maps and densities of built-up use and land surface temperature maps

	Densities of urban/built-up use			Land surface temperatures	
	Road buffer	Liwan buffer	Yuanchun buffer	1989 map	1997 map
SO_2	0.33	0.65	0.76	0.54	0.67
NO_x	0.69	0.39	0.42	0.68	0.72
Dust	0.53	0.64	0.68	0.36	0.44

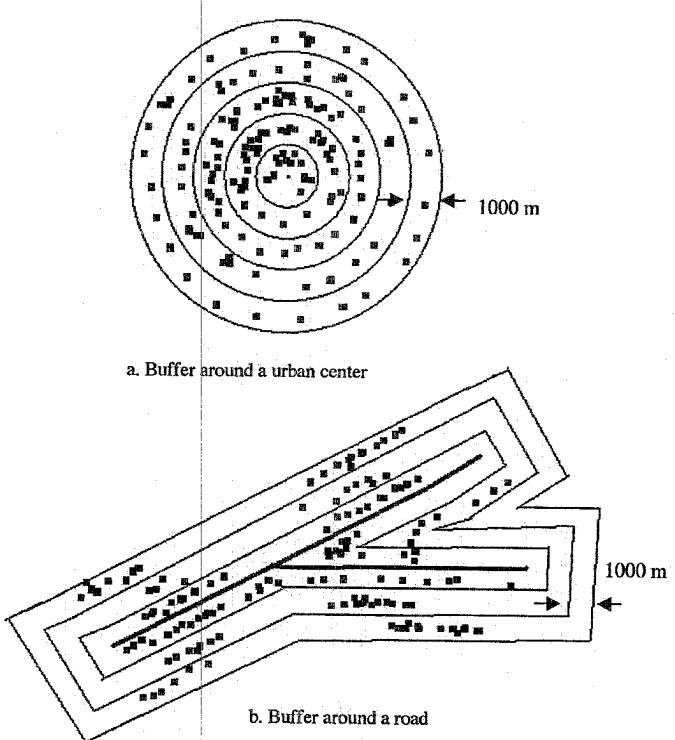

Figure 8. A diagram illustrating how the densities of urban/built-up land are calculated within the buffer zones using GIS.

Table II shows the results of correlation analyses. For SO_2, a correlation coefficient value of 0.33 was obtained (significant level of 0.05) with the road buffer as the overlay layer, while a coefficient value of 0.65 and 0.76 was found respectively with the Liwan buffer and the Yuanchun buffer as the overlay layer. This finding suggests that the spatial distribution of SO_2 concentration was significantly

related to the distance from the pollution centers, but showed little relation with the distance from the major road network. The results of correlation analysis for NO_x were contrastingly different from those of SO_2. A coefficient value of 0.69 was observed with the road buffer zones as statistical units, indicating that the mapped pattern of NO_x was closely associated with that of sectoral urban expansion. Much weaker correlation was found with the Liwan buffer ($r = 0.39$) and Yuanchun buffer ($r = 0.42$) as GIS overlays. These computations confirm our observation that NO_x was a more traffic related rather than a built-up related pollution. Higher concentrations were observed along major radial transportation routes, such as eastward development along the Guang-Shen Expressway and the Guang-Jiu Railway, southward development along the Guangzhou Da Road and Guang-Pan Highway, and recent northwestward development and northeastward development. Correlations between the densities of urban/built-up land and dust concentrations suggest that the pattern of dust pollution possessed a stronger linkage to pollution centers such as Liwan ($r = 0.64$) and Yuanchun ($r = 0.68$) than to the transportation network ($r = 0.53$). The concentrations of dust in the city conformed more to the pattern of concentric zonation, and less to the pattern of sectoral radiation.

6. Urban Thermal Patterns and Air Pollution

A choropleth map (Figure 9) was produced to show the spatial distribution of emissivity- corrected LSTs in 1989 and 1997. The statistics of LST on December 13, 1989 indicates that the lowest temperature was 16.98 °C, the highest temperature 25.23 °C, and the mean 21.17 °C, with a standard deviation of 1.72. From Figure 9, it becomes apparent that all the urban or built-up areas have a relatively high temperature. Some "hot spots" (the highest temperature class) can be clearly identified. In 1989, the most extensive hot spot was found in the western part of Haizhu District, an industrial region in the city. Another noticeable hot spot was detected in the southeast corner of the city proper, where Guangzhou Economical and Technological Development Zone is located. There were also many small hot spots throughout the Tianhe District, which are related to the sparsely distributed industries in the region. However, there was not an extensive hot spot in the old urban areas such as Liwan, Yuexiu, and Dongshan Districts, in spite of their high construction density. Apparently, commercial and residential areas are less effective to increase land surface temperature. The lowest temperature class (16.98–19.45 °C) appeared in the following three areas: (1) The eastern part of Baiyun District around Maofeng Mountain; (2) Baiyun Hill; and (3) The southeastern part of Haizhu District. These areas were substantially rural at one time, and were mostly covered by forest. Both the northwest Baiyun District and west Fangcun District have a moderate temperature ranging from 19.45 °C to 21.17 °C, where cropland and dike-pond land prevailed.

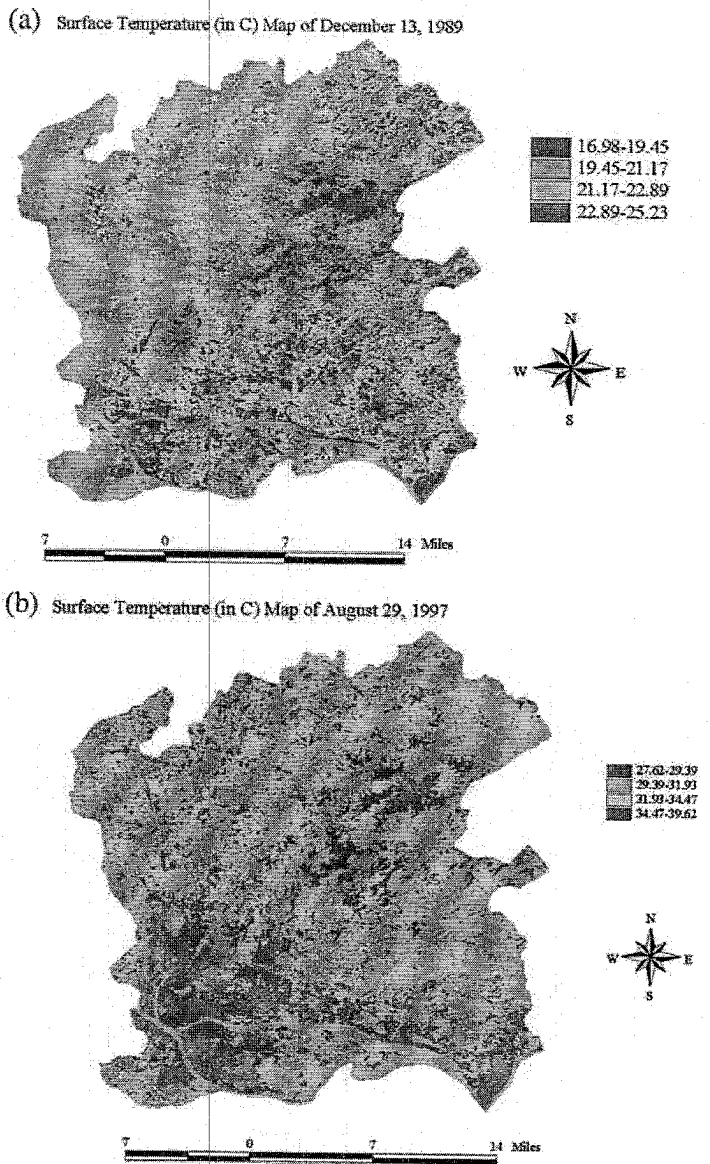

Figure 9. A choropleth map showing the geographical distribution of land surface temperature in 1989 and 1997.

The spatial pattern of LST on August 29, 1997 is markedly different from that of December 13, 1989, as seen from Figure 9. The difference reflects not only the differences in solar illumination, the state of vegetation, and atmospheric influences of remotely sensed TM data set, but also changes in land use and land cover. The 1997 image was taken in the hottest month. The average temperature was 31.93 °C, with a range between 27.62 °C and 39.62 °C. The standard deviation was also larger (2.54 °C) than that in 1989, indicating that the surfaces experienced a wider variation in LST. The urban and rural areas can easily be distinguished from Figure 9. The urban areas showed a high temperature of over 34.47 °C, while the rural settlements a minimal temperature of 31.93 °C. A major hot spot expanded eastward from the urban core areas of Liwan, Yuexiu, Dongshan to Huangpu, forming a high temperature corridor. A major hot spot to the south of the Pearl River seemed to stretch out from the western Haizhu to Fangcun District. In addition, two large hot spots newly emerged, one centered at Guangzhou Railroad Station and Baiyun International Airport, and the other to the east of Baiyun Hill. Both areas had undergone a rapid urban sprawl since the 1990s. Numerous strip-shaped hot spots were also detectable along the northward highways such as Guangzhou-Huaxian, Guangzhou- Huandong, and Guangzhou-Conghua Highways.

The relationship between the LST maps and three concentration maps (SO_2, NO_x, and Dust) was investigated through a pixel-by-pixel correlation analysis, after converting the concentration maps into raster format with a grid resolution of 30 meters. The significance of each correlation coefficient was determined using a one-tail Student's t-test. It is found that the concentrations of the pollutants tended to positively correlate with LST values in both years, but exhibited a stronger correlation with the 1997 (summer LST) map (Table II). The highest positive correlation was found in NO_x (0.72 with the 1997 LST map, and 0.68 with the 1989 map). In both years, SO_2 exhibit a moderate correlation with LST (0.67 for 1997 and 0.54 for 1989). An even lower correlation was observed in the concentrations of dust of the both years (0.44 in 1997 and 0.36 in 1989). This study has re-confirmed the existence of the relationship between pollutant measurements and LSTs, and the mechanisms of this correlation warrant further investigations. Previous studies suggest that the distinctive LST patterns are associated with the thermal characteristics of land cover classes (Weng, 2003; Weng *et al.*, 2004). Moreover, land use zoning has demonstrated to have a profound impact on the physical characteristics of urban land covers by imposing such restrictions as maximum building height and density, the extent of impervious surface and open space, land use types and activities. These restrictions would impact surface energy exchange, surface and subsurface hydrology, micro- to meso-scale weather and climate systems, and other environmental processes (Wilson *et al.*, 2003). Apparently, knowledge about the interplay among land use, land cover, air pollution, and thermal landscape should be integrated in order to assess the causes of the relationship between remote sensing derived measurements and air pollution concentrations.

7. Conclusion

This study suggests that high-quality data and reliable information regarding to land use, land cover, and LST can be derived with satellite remote sensing and GIS technologies, and that the data so derived closely corresponded to ambient air quality measurements. The spatial patterns of air pollution is subject to the influence of many factors related to land use activities, such as the division of functional districts, the distribution of land use types, the occurrence of water bodies and parks, building and population densities, the layout of transportation network, and air flushing rates. In the Guangzhou context, the impact of these factors varied with different pollutants, and the street canyon effect was particularly evident due to its closely spaced high- rise buildings and low-wind environment. Because of the locations of industrial plants, high population density, clustering of catering industry, and low air flushing rates, two urban localities (namely, Liwan and Yuanchun) became the pollution hubs of SO_2, Dust, and other pollutants. The study demonstrates that GIS is effective in examining the spatial pattern of air pollution and its association with urban built-up density. Positive correlation between the concentrations of the pollutants probed and satellite derived LST values, particularly with the summer LST map, indicates that both ambient air quality and LST were associated with land use. This linkage is apparently complex, given the fact that it involves multiple variables and varies with the environmental and socio-economic settings of cities under investigation. Further studies of the linkage are warranted, noting that it may occur at different spatial and temporal scales.

The accuracy of pollutant maps is of particularly significant in this type of analysis, since they would influence the correlation analyses between the pollutants and urban built-up densities/LSTs. In this study, the maps were produced by the city's environmental monitoring authority based on data collected in the fixed and mobile observations. Contours were drawn by interpolation of point data, which represented annual averages of pollutant measurements. The contours were manually digitized as vector GIS data layers. To examine the relationship between the pollutants and urban built-up densities, a vector GIS analysis was conducted after computing the densities of urban/built-up within buffer zones. On the other hand, in analyzing the relationship between the pollutants and surface temperatures, a raster GIS approach was applied by converting the pollutant maps into the raster format and conducting a pixel-by-pixel correlation analysis. Data conversion between the vector and raster format tends to introduce error. This error will be augmented in the process of analysis where two or more data layers are used. Error propagation modeling and sensitivity analysis should be conducted in the future research of similar types.

Satellite thermal infrared (TIR) sensors measure top of the atmosphere (TOA) radiances, from which brightness temperatures can be derived using Plank's law (Dash *et al.*, 2002). The TOA radiances are the mixing result of three fractions

of energy: (1) emitted radiance from the Earth's surface; (2) upwelling radiance from the atmosphere; and (3) downwelling radiance from the sky. The difference between the TOA and land surface brightness temperatures ranges generally from 1 to 5 K in the 10–12 μm spectral region, subject to the influence of the atmospheric conditions (Prata *et al.*, 1995). Therefore, atmospheric effects, including absorption, upward emission, and downward irradiance reflected from the surface (Franca and Cracknell, 1994), must be corrected before land surface brightness temperatures are obtained. Further studies are therefore needed to determine the impact of the presence of a pollution layer on the three types of atmospheric effects, as well as their aggregated effect. Moreover, from remote sensing perspective, how pollutants are sensed in the TIR channel(s), visible, and near-mid infrared channels of a sensor is certainly a significant issue to be examined in the future. In addition, accurate LST measurements require the brightness temperatures to be further corrected with spectral emissivity values. This correction is imperative for a scientific assessment of the relationship between LSTs and air quality measurements.

Acknowledgments

The authors thank the National Geographic Society for sponsoring this research through a grant (Grant number: 6811-00). Research assistance given by Ms. Bingqing Liang is greatly acknowledged. The constructive comments and suggestions of the anonymous reviewers help improving this paper.

References

Anderson, J. R., Hardy, E. E., Roach, J. T. and Witmer, R. E.: 1976, *A Land Use and Land Cover Classification Systems for Use with Remote Sensing Data*, USGS Professional Paper, p. 964.

Artis, D. A. and Carnahan, W. H.: 1982, 'Survey of emissivity variability in thermography of urban areas', *Remote Sens. Environ.* **12**, 313–329.

Balling, R. C. and Brazell, S. W.: 1988, 'High resolution surface temperature patterns in a complex urban terrain', *Photogramm. Eng. Rem. S.* **54**, 1289–1293.

Brivio, P. A., Gempvese, G., Massari, S., Mileo, N., Saura, G. and Zilloli, E.: 1995, 'Atmospheric pollution and satellite remotely sensed surface temperature in metropolitan areas', in: EARSeL (ed), *EARSeL Advances in Remote Sensing Pollution Monitoring and Geographical Information Systems*, Paris, pp. 40–46.

Byrne, G. F.: 1979, 'Remotely sensed land cover temperature and soil water status – A brief review', *Remote Sens. Environ.* **8**, 291–305.

Carnahan, W. H. and Larson, R. C.: 1990, 'An analysis of an urban heat sink', *Remote Sens. Environ.* **33**, 65–71.

Carson, T. N., Gillies, R. R. and Perry, E. M.: 1994, 'A method to make use of thermal infrared temperature and NDVI measurements to infer surface soil water content and fractional vegetation cover', *Remote Sens. Rev.* **9**, 161–173.

Dash, P., Gottsche, F.-M., Olesen, F.-S. and Fischer, H.: 2002, 'Land surface temperature and emissivity estimation from passive sensor data: Theory and practice-current trends', *Int. J. Remote Sens.* **23**, 2563–2594.

DeWitt, J. and Brennan, M.: 2001, 'Taking the Heat', *Imaging Notes*, **16**(6), 20–23.

Franca, G. B. and Cracknell, A. P.: 1994, 'Retrieval of land and sea surface temperature using NOAA-11 AVHRR data in north-eastern Brazil', *Int. J. Remote Sens.* **15**, 1695–1712.

Gallo, K. P. and Owen, T. W.: 1998, 'Assessment of urban heat island: A multi-sensor perspective for the Dallas-Ft. Worth, USA region', *Geocarto Int.* **13**, 35–41.

Gallo, K. P., McNab, A. L., Karl, T. R., Brown, J. F., Hood, J. J. and Tarpley, J. D.: 1993, 'The use of NOAA AVHRR data for assessment of the urban heat island effect', *J. Appl. Meteorol.* **32**, 899–908.

Gibbons, D. E. and Wukelic, G. E.: 1989, 'Application of Landsat Thematic Mapper data for coastal thermal plum analysis at Diablo Canyon', *Photogramm. Eng. Rem. S.* **55**(6), 903–909.

Gillies, R. R. and Carlson, T. N.: 1995, 'Thermal remote sensing of surface soil water content with partial vegetation cover for incorporation into climate models', *J. Appl. Meteorol.* **34**, 745–756.

Gillies, R. R., Carlson, T. N., Cui, J., Kustas, W. P. and Humes, K. S.: 1997, 'A verification of the 'triangle' method for obtaining surface soil water content and energy fluxes from remote measurements of the Normalized Difference Vegetation index (NDVI) and surface radiant temperature', *Int. J. Remote Sens.* **18**, 3145–3166.

Goward, S. N., Xue, Y. and Czajkowski, K. P.: 2002, 'Evaluating land surface moisture conditions from the remotely sensed temperature/vegetation index measurements: An exploration with the simplified simple biosphere model', *Remote Sens. Environ.* **79**, 225–242.

Guangdong Statistical Bureau: 1999, *Guangdong Statistical Yearbook*, China Statistics Press, Beijing. (in Chinese).

Guangzhou Bureau of City Planning: 1996, *Master Plan of Guangzhou City, 1991–2010 (Guangzhou Shi Chengshi Zongti Guihua)*, Guangzhou Bureau of City Planning, Guangzhou, China. (in Chinese).

Guangzhou City Local Chronicle Compilation Committee (GZCLCCC): 1995, *Gazetteer of Guangzhou (Volume Three)*, Guangzhou Press, Guangzhou. (in Chinese).

Guangzhou Municipality Planning Committee: 1997, *Atlas of Guangzhou Natural Resources*, Guangdong Province Atlas Publishing House, Guangzhou. (in Chinese).

Guangzhou Statistical Bureau: 1999, *Fifty Years in Guangzhou, 1949–1999*, China Statistics Press, Beijing. (in Chinese).

Guo, H.: 2001, '*Land* Use and Land Cover Changes and Environmental Impacts in Guangzhou', *Master Thesis*, Department of Geography, South China Normal University, Guangzhou, China. (in Chinese).

Kidder, S. Q. and Wu, H. T.: 1987, 'A multispectral study of the St. Louis area under snow-covered conditions using NOAA-7 AVHRR data', *Remote Sens. Environ.* **22**, 159–172.

Kim, H. H.: 1992, 'Urban heat island', *Int. J. Remote Sens.* **13**, 2319–2336.

Malaret, E., Bartolucci, L. A., Lozano, D. F., Anuta, P. E. and McGillem, C. D.: 1985, Landsat-4 and Landsat-5 Thematic Mapper data quality analysis, *Photogramm. Eng. Rem. S.* **51**, 1407–1416.

Markham, B. L. and Barker, J. K.: 1985, 'Spectral characteristics of the LANDSAT Thematic Mapper sensors', *Int. J. Remote Sens.* **6**, 697–716.

Marsh, W. M. and Grossa, J. M. Jr.: 2002, *Environmental Geography: Science, Land Use, and Earth Systems*, 2nd edition, John Wiley and Sons, New York.

Nichol, J. E.: 1994, 'A GIS-based approach to microclimate monitoring in Singapore's high-rise housing estates', *Photogramm. Eng. Rem. S.* **60**, 1225–1232.

Nichol, J. E.: 1996, 'High-resolution surface temperature patterns related to urban morphology in a tropical city: A satellite-based study', *J. Appl. Meteorol.* **35**(1), 135–146.

Oke, T. R.: 1982, 'The energetic basis of the urban heat island', *Quart. J. Royal Meteorol. Soc.* **108**, 1–24.

Poli, U., Pignatoro, F., Rocchi, V. and Bracco, L.: 1994, 'Study of the heat island over the city of Rome from Landsat-TM satellite in relation with urban air pollution', in: R. Vaughan (ed), *Remote Sensing – From Research to Operational Applications in the New Europe*, Springer Hungarica, Berlin, pp. 413–422.

Prata, A. J., Caselles, V., Coll, C., Sobrino, J. A. and Ottle, C.: 1995, 'Thermal remote sensing of land surface temperature from satellites: Current status and future prospects', *Remote Sens. Rev.* **12**, 175–224.

Qian, Z., Zhang, J., Wei, F., Wilson, W. E. and Chapman, R. S.: 2001, 'Long-term ambient air pollution levels in four Chinese cities: Inter-city and intra-city concentration gradients for epidemiological studies', *J. Expos. Anal. Environ. Epidemiol.* **11**, 341–351.

Quattrochi, D. A. and Luvall, J. C.: 1999, *High Spatial Resolution Airborne Multispectral Thermal Infrared Data to Support Analysis and Modeling Tasks in the EOS IDS Project ATLANTA*, URL: http://wwwghcc.msfc.nasa.gov/atlanta/, Global Hydrology and Climate Center, NASA, Huntsville, Alabama (last date accessed: 26 June 2005).

Quattrochi, D. A. and Ridd, M. K.: 1994, 'Measurement and analysis of thermal energy responses from discrete urban surfaces using remote sensing data', *Int. J. Remote Sens.* **15**(10), 1991–2022.

Roth, M., Oke, T. R. and Emery, W. J.: 1989, 'Satellite derived urban heat islands from three coastal cities and the utilisation of such data in urban climatology', *Int. J. Remote Sens.* **10**, 1699–1720.

Streutker, D. R.: 2002, 'A remote sensing study of the urban heat island of Houston, Texas', *Int. J. Remote Sens.* **23**, 2595–2608.

Streutker, D. R.: 2003, 'Satellite-measured growth of the urban heat island of Houston, Texas', *Remote Sens. Environ.* **85**, 282–289.

Voogt, J. A. and Oke, T. R.: 2003, 'Thermal remote sensing of urban climate', *Remote Sens. Environ.* **86**, 370–384.

Wang, S., Shao, M. and Zhang, Y.: 2001, 'Influence of fuel quality on vehicular NO_x emissions', *J. Environ. Sci.* **13**(3), 265–271.

Ward, L. and Baleynaud, J.-M.: 1999, 'Observing air quality over the city of Nates by means of Landsat thermal infrared data', *Int. J. Remote Sens.* **20**(5), 947–959.

Weng, Q.: 2001, 'A remote sensing-GIS evaluation of urban expansion and its impact on surface temperature in the Zhujiang Delta, China', *Int. J. Remote Sens.* **22**, 1999–2014.

Weng. Q.: 2003, 'Fractal analysis of satellite-detected urban heat island effect', *Photogramm. Eng. Rem. S.* **69**, 555–566.

Weng, Q., Lu, D. and Schubring, J.: 2004, 'Estimation of land surface temperature-vegetation abundance relationship for urban heat island studies', *Remote Sens. Environ.* **89**(4), 467–483.

Wilson, J. S., Clay, M., Martin, E., Stuckey, D. and Vedder-Risch, K.: 2003, 'Evaluating environmental influences of zoning in urban ecosystems with remote sensing', *Remote Sens. Environ.* **86**, 303–321.

Xie, M. and Chen, N.: 2001, 'Changes in Guangzhou's air pollution and strategies for control them based on an analysis of changes in the sanitary district', Unpublished paper, Guangzhou Municipality Environmental Monitoring Central Station, Guangzhou, China.

Xie, S., Zhang, Y., Li, Q. and Tang, X.: 2003, 'Spatial distribution of traffic-related pollution concentrations in street canyons', *Atmos. Environ.* **37**, 3213–3224.

Xu, J.: 1990, *A Collection of Essays on Lingnan Historical Geography (Lingnan Lishi Dili Lunji)*, Zhongshan University Press, Guangzhou. (in Chinese).

Xu, X.: 1985, 'Guangzhou: China's Southern Gateway', in: Victor F.S. Sit (ed), *Chinese Cities: The Growth of the Metropolis Since 1949*, Oxford University Press, Hong Kong.

Zhang, Y., Xie, S., Zeng, L. and Wang, H.: 1999, 'Traffic emission and its impact on air quality in Guangzhou area', *J. Environ. Sci.* **11**(3), 355–360.